MASTER

PREPRINT UCRL- 78044 Rev. 1

CONF-761108--9

Lawrence Livermore Laboratory

SCATTERED LIGHT EVIDENCE FOR SHORT DENSITY SCALE HEIGHTS NEAR CRITICAL DENSITY IN LASER-IRRADIATED PLASMAS

D. W. Phillion, R. A. Lerche, V. C. Rupert, R. A. Haas, and M. J. Boyle

September 15, 1976

This paper was prepared for submission to the APS Meeting, San Francisco, California, November 15-19, 1976

This is a preprint of a paper intended for publication in a journal or proceedings. Since changes may be made before publication, this preprint is made available with the understanding that it will not be cited or reproduced without the permission of the author.

SCATTERED LIGHT EVIDENCE FOR SHORT DENSITY SCALE HEIGHTS NEAR CRITICAL DENSITY IN LASER-IRRADIATED PLASMAS

D. W. Phillion, R. A. Lerche, V. C. Rupert, R. A. Haas, and M. J. Boyle

Lawrence Livermore Laboratory
University of California
Livermore, California 94550

NOTICE
This report was prepared as an account of work sponsored by the United States Government. Neither the United States nor the United States Energy Research and Development Administration, nor any of their employees, nor any of their contractors, subcontractors, or their employees, makes any warranty, express or implied, or assumes any legal liability or responsibility for the accuracy, completeness or usefulness of any information, apparatus, product or process disclosed, or represents that its use would not infringe privately owned rights.

ABSTRACT

We present experimental evidence of a steepened electron density profile near critical density obtained from studying the time-integrated scattered light from targets illuminated by linearly polarized, 1.06 μ light. Both 10 μ thick disks and DT-filled glass microshells were irradiated by light focused by f/1 or f/2.5 lenses in one and two-beam experiments, respectively. From the dependence of the asymmetry of the scattered light about the beam axis upon the scattering angle, we infer scale lengths on the order of one micron. Scale lengths have also been deduced from measurements on the polarization state of the reflected light. Both analytic and numerical results are presented to show how the polarization state varies with the incidence angle and the scale length.

---

* Work performed under the auspices of the U. S. Energy Research and Development Administration under contract no. W-7405-Eng-48.

DISTRIBUTION OF THIS DOCUMENT IS UNLIMITED

SCATTERED LIGHT EVIDENCE FOR SHORT DENSITY SCALE HEIGHTS NEAR CRITICAL DENSITY IN LASER-IRRADIATED PLASMAS

D. W. Phillion, R. A. Lerche, V. C. Rupert, R. A. Haas, and M. J. Boyle

I. INTRODUCTION

Direct evidence of short density scale heights near critical density has been obtained from measurements of the polarization of the light scattered by laser-fusion targets. Additionally, short scale lengths have been inferred from studying the time-integrated angular distribution of scattered light at the laser wavelength (1.064μ) on the premise that any azimuthal asymmetry about the beam axis is due to resonance absorption. The experiments were carried out on the CYCLOPS[1] and ARGUS[2] laser-irradiation facilities on single-beam-irradiated, tungsten-glass and parylene disks and two-beam-irradiated, DT-filled, glass microballoons.

II. POLARIMETRY MEASUREMENTS ON THE SCATTERED LIGHT

The electromagnetic field equations describing a monochromatic plane wave obliquely incident upon a plane-stratified plasma with density variations along only a single direction z, may be divided into two uncoupled groups of equations. Choosing the x axis to be perpendicular to the plane formed by the z axis and the propagation direction of the incident wave, then E_x, H_y, H_z are the field components for the TE or s-polarized wave and H_x, E_y, E_z are the TM or p-polarized wave components. The reflection coefficients for the two plane wave components will differ both in amplitude and phase since the

wave equation for H_x has a term proportional to the product of the first derivatives of the election density and the field, which does not appear in the wave equation for E_x[3]. By measuring the polarization state of the reflected wave and assuming a shape for the plasma density profile, a characteristic density scale length may be deduced.

The two extreme limiting cases are shown in figure 1. In the geometrical optics limit, the density gradient is assumed to be vanishingly small. The equation of motion[4] for the electric polarization unit vector $\hat{e}$ may be expressed in terms of the eikonal ζ and the refractive index n:

$$\frac{d\hat{e}}{d\tau} = - (\hat{e} \cdot \text{grad } \log_e n) \text{ grad } \zeta, \qquad (1)$$

where τ is the optical path length integrated along the ray trajectory. Since grad ζ always lies in the scattering plane, we find by taking the dot product of Eq. (1) with the normal vector to this plane that $\hat{e}$ will remain at a constant angle to the plane. In the metal limit, the density discontinuously jumps from vacuum to infinite density. On the surface of discontinuity, the tangential electric field must be zero. Upon reflection, $\hat{e}$ will thus be inverted so that it projects below the scattering plane. The disparity between the limits is maximum when Ψ equals 45°. At this angle, the incident wave is an equal-amplitude superposition of TE and TM waves.

The polarimeters used in the experiments described here did not make a complete measurement of the polarization state, but only measured the time-averaged degree of linear polarization along an axis. The polarimeter was constructed (figure 2) so that two photodiodes measured both the light reflected from and the light transmitted through a 1mm thick window at Brewster's angle to the scattered light. The reflections from the glass

surfaces added incoherently for two reasons: firstly, the two reflections were temporally incoherent since they arrived at the detector separated by ten picoseconds. Others[5] have found the scattered light to have a spectrum typically many angstroms wide. Secondly, the two reflections are spatially incoherent due to a large angular field of view one degree in diameter. From these measurements, the degree of linear polarization $p = (I_{\parallel}-I_{\perp})/(I_{\parallel}+I_{\perp})$ was calculated, where $I_{\parallel}$ and $I_{\perp}$ were the energy flux densities of the light polarized parallel to and perpendicular to the transmission axis of the Brewster window, respectively. Preceeding the splitter in the beam path were a 100 Å bandpass interference filter centered at the laser wavelength, a neutral density filter, and, in the ARGUS experiments, a Pb-glass filter to block superthermal x-rays. The polarimeter was oriented so that its transmission axis projected out of the scattering plane at an angle of 45°. The TM wave is assumed to have been attenuated by a factor α and retarded in phase by δ relative to the TE wave. For the metal limit where $\alpha = 1$ and $\delta = 180°$, the resultant wave is linearly polarized along the transmission axis. More generally, the intensity components are

$$I_{\parallel} = 1/4 \mid 1 + \alpha e^{i\delta}\mid^2 \quad \text{and} \quad I_{\perp} = 1/4 \mid 1 - \alpha e^{i\delta}\mid^2, \qquad (2)$$

giving for the degree of linear polarization:

$$p = \left(\frac{2\alpha}{1+\alpha^2}\right) \quad (-\cos\delta) \qquad (3)$$

Setting the first factor equal to one in Eq. (3) is not a bad approximation since even if the TM wave undergoes 50% resonant absorption, this factor is only reduced to 0.94.

Before the measurement of p can be translated into a density scale height L, a specific density profile must be assumed. We assume the electron density increases linearly with distance from a sub-critical density n_L to a super-critical density n_H with a slope $L^{-1} = d(n/n_{crit})/dz$. The electron density decreases from n_L to vacuum density with vanishingly small slope on the one side and remains constant at n_H on the other.

The TE and TM wave equations were integrated numerically between the limits n_L and n_H, starting from the high density boundary, where the tangential electric and magnetic field components were matched to an evanescent wave on the constant density side. The incident and reflected wave amplitudes were obtained by again matching tangential field components at the low density boundary. The step size was computed at each step by solving for the characteristic spatial frequencies of the second order difference equation replacing the wave equation in the numerical integration, assuming its coefficients not to be rapidly varying. The step size was made equal to a small number ε ($\varepsilon \leq 0.01$) divided by the greater of the two moduli of the characteristic frequencies. This insured the fractional change in the wave function in each iteration would be of order ε. This strategem was necessary because of the singularity at critical density in the TM wave equation. The singularity was removed by assuming a phenomenological electron-ion collision frequency ν given by:

$$\frac{\nu}{\omega} = 10^{-3} \frac{n}{n_c} \qquad (4)$$

Provided ν/ω is small, the relative phase retardation and attenuation are insensitive to the choice for ν. From the curve in Figure 3a for which $(n_L, n_H) = (0.5\ n_c, 2.0\ n_c)$, and $\theta = 22.5°$, we

read a phase retardation $\delta = 96.64°$ for a scale length of 1.5 λ_o. If ν/ω were chosen to be 10^{-5} at critical density instead of 10^{-3}, then δ would be 96.67°, while for $\nu/\omega = 0.1$, $\delta = 96.21°$.

The phase retardation is plotted as a function of the scale length with the angle of incidence θ as a parameter in figure 3 for two combinations of (n_L, n_H); namely, $(0.5n_c, 2.0n_c)$ and $(0.75n_c, 1.25n_c)$. This angle is measured between the propagation direction of the incident beam in vacuum and the density gradient. The phase retardation δ does not approach 180° in the limit of a discontinuous jump since the magnitude of the jump is finite. In the step limit, δ can be found from the Fresnel formula:[6]

$$\tan \frac{\delta}{2} = \frac{\cos\theta_1 \sqrt{\sin^2\theta_1 - \left(\frac{n_2}{n_1}\right)^2}}{\sin^2\theta_1} \qquad (5)$$

where n_1, n_2 are the indices of refraction on the low and high density sides of discontinuity, respectively, and θ_1 is obtained from the incidence angle θ_o by Snell's law:

$$\theta_1 = \sin^{-1}\left(\frac{\sin\theta_o}{n_1}\right) \qquad (6)$$

Two-beam experiments on 100μ-diameter, DT-filled glass microspheres were carried out on the two-terrawatt ARGUS facility with an oscillator pulse duration of about 30 psec FWHM. Two polarimeters looked at the light backscattered at angles of 45° to the two opposing beams. Their orientation and location in the target chamber were as described by figure 2. The beams were focussed onto the target so that 90% of the energy was contained in a cone of 19° half-angle, and were made nearly circular by removing the astigmatism with an adjustable corrector. It's assumed

here that most of the light each polarimeter saw originated from the beam nearest it. But for shot #36080406, the great energy imbalance between the two arms made it nearly a one-beam shot and thus for this shot there is no such confusion. Table I summarizes the polarimetry measurements obtained in the ARGUS ball-on-stalk experiments. The range of incidence angles in figure 3a is intended to indicate the measurement uncertainties associated with the finite angular width of the incident beam. If the polarimeters saw light originally incident on-axis, the density scale height must have been less than one micron and the magnitude of the density jump must have exceeded $n_c/2$.

III. SPATIAL DISTRIBUTION OF THE SCATTERED LIGHT

Study of the spatial distributions of the scattered light and particle blowoff from the laser-produced plasma is essential to understanding the stimulated scattering and collective absorption processes which determine both the fraction of light absorbed and where and how it is deposited into the plasma. Large azimuthal asymmetries in the scattered light have always been observed, but azimuthal asymmetries in the energy of the particle blow-off have only been observed for experiments on DT-filled glass microsphere targets and not for experiments on disk targets. At a given polar angle (angle made by the detector line-of-sight with the beam axis), light preferentially scatters in a plane which is perpendicular to the laser electric field (out-of-plane scattering), while the most energetic particle blowoff usually occurs in the plane of polarization formed by the electric field and propagation directions of the incident beams (in-plane scattering). If it is assumed that the particle blowoff is more or less directed radially outward, the ion calorimetry results then imply those sectors of the ball

where the light was incident as a p-polarized wave were preferentially heated. Figure 4 shows the in and out-of-plane polar distributions of both the scattered light and particle blowoff energies for a DT-filled glass microsphere target shot on the ARGUS facility.

The calorimeters[8] are of a differential design in which a central circular metal receiver completely absorbs the x-ray and particle blowoff energies but only seven percent of the scattered light. A surrounding annular metal receiver concentric with and of equal area to the central receiver sees only the scattered light, since it is shielded by a sheet of pyrex. Thermoelectric modules are used to measure the temperatures of the receivers with respect to a common reference. The temperature difference is proportional to the energy carried by x-rays and particles. Stimulated Brillouin sidescatter (SBS) can easily explain the asymmetric scattered light distribution, since it preferentially scatters light normal to the electric field of the incident light,[9] but an explanation of the asymmetric particle blowoff distribution in terms of SBS rather than resonance absorption would have to assume SBS is more efficient in the out-of-plane sectors.

Ball-on-stalk experiments conducted on the CYCLOPS two-beam irradiation facility with f/2.5 lenses also showed a strong polarization dependence in the scattered light (Figure 5a) , but the ion calorimetry results were anomalous, showing that the particle blowoff was most energetic out of the plane of polarization. Non-axisymmetric heating of the ball may have been directly confirmed by photographs of the time-integrated x-ray emission imaged by a microscope. The camera viewed the target along a line of sight that lay in the plane of polarization and was at an angle of 45° to the beam axis. Photograph B in Figure 5b shows the brightness to be greatest for those sectors where the light was incident

as a p-polarized wave. This does not necessarily mean these sectors also emit x-ray more intensely: the azimuthal asymmetry may simply be a consequence of the viewing direction.

The azimuthal asymmetry of the scattered light distribution for ball-on-stalk targets has been observed to generally increase with intensity. An averaged scattered light intensity distrubution for the JANUS two-beam experiments on 80μ diameter glass microspheres is shown in Figure 6. The scattered energy in joules per steradian has been normalized to the total incident energy, which was typically 35J in 75 psec. The intensities averaged about $2 \cdot 10^{15}$ W/cm^2, compared to $3 \cdot 10^{15}$ W/cm^2 for the Cyclops shot #56020501 (Figure 5a) and $6.7 \cdot 10^{15}$ W/cm^2 for ARGUS shot #36080507 (Figure 4). The intensity of the light scattered out-of-plane is only about 25% greater than that scattered in-plane. The ion calorimetry data indicates an azimuthal variation opposite to what is observed for the light. Interpretation of this data is complicated by the ion calorimeters being positioned at different polar angles as well as at different azimuths. Simulations by LASNEX,[10] a two-dimensional hydrodynamics code which demands axial symmetry, predict the ratio of the two data points to be about 4/3 rather than the 3 to 1 average value observed.

In one-beam experiments with lead-glass disks[11] on CYCLOPS, the azimuthal variation of the scattered light intensity was studied by a ring of twelve equally-spaced diodes looking at the light backscattered at an angle of 26° to the incident beam. Figure 7 shows the polarization dependence to be dramatic. Both these shots were for nominally 400μ spot diameters and 100 psec pulse widths, giving intensities of $10^{14} \rightarrow 10^{15}$ W/cm^2. Such large azimuthal asymmetries of several-to-one make resonance absorption difficult to accept as an explanation, since for a linear density profile, the maximum amount of resonant absorption that can occur for any scale length or any incidence angle is about 50 percent.

Once the requirement of a linear density profile is abandoned, resonant absorption can become extremely efficient. J. M. Kindel, K. Lee, and E. L. Lindman[12] have observed greater than 90% absorption in one-dimensional collisionless plasma simulations with fixed ions for a class of two-step density profiles. However, in two-dimensional, relativistic particle and electromagnetic field simulations with mobile ions using the code ZOHAR, K. G. Estabrook, E. J. Valeo, and W. L. Kruer[12] found no greater than 60% absorption after the density profile had evolved to steady-state. Thus SBS seems the more reasonable explanation to us. Preferential scattering out of the plane of polarization has been seen in two-dimensional, one-fluid simulations done by Kent Estabrook.[13]

The polar dependence of the azimuthal asymmetry of the scattered light for a tungsten-glass disk target is shown by Figure 8. If the azimuthal asymmetry were due solely to resonance absorption, the asymmetry should have vanished both for direct backscatter and for sidescatter at large angles away from the beam axis. Instead the asymmetry becomes progressively greater as one looks at the angles further from the beam axis. However, failure of the critical density surface to a surface of revolution about the beam axis could also cause an asymmetry in the scattered light. From Figure 3b, which shows how the azimuthal asymmetry due to resonance absorption varies with incidence angles and density scale length, a density scale height on the order of one micron can be inferred from the lack of asymmetry at $\theta = 164°$ and the asymmetry of $I_{\parallel} / I_{\perp} = 0.62$ at $\theta = 150°$. The incidence angle θ in Figure 36 equals $(180° - \theta)/2$, where θ here is the polar angle of the scattered light in Figure 8. Direct backscatter corresponds to a polar angle $\theta = 180°$.

IV. ACKNOWLEDGEMENTS

One of the authors is grateful for the many discussions with W. L. Kruer which contributed greatly to his understanding. Acknowledgement is also due E. K. Storm, K. R. Manes, K. M. Brooks, D. R. Speck, F. Rainer and many others for performing the experiments.

REFERENCES

1. D. R. MacQuigg, D. R. Speck, "Beam Diagnostics on ARGUS" LLL UCRL-78447, November, 1976.

2. D. R. Speck and W. W. Simmons, "Argus Laser Fusion Facility", 1976 APS meeting in San Francisco, Ca. UCRL #78438.

3. V. L. Ginsbury, "The Propagation of Electromagnetic Waves in Plasmas, 2nd Edition", (Pergamon Press, Oxford, 1966), p. 260.

4. Max Born and Emil Wolf, "Principles of Optics, 4th Edition" (Pergamon Press, Oxford, 1970), p. 119.

5. L. M. Goldman, J. Soures, and M. J. Lubin, "Saturation of Stimulated Backscattered Radiation in Laser Plasmas", Phys. Rev. Lett. 31, 1184 (1973).

6. J. A. Stratton, "Electromagnetic Theory" (McGraw-Hill, New York, 1941), p. 500.

7. E. K. Storm, "Exploding Pusher Targets at 2 TW", to be presented at 1976 APS meeting in San Francisco, Ca. UCRL #78414.

8. S. R. Gunn and V. Rupert, UCRL in preparation.

9. J. M Dawson and A. T. Lin, "Parametric Instabilities in Plasma", Dept. of Physics, Univ. of Ca. at Los Anglees, report PPG-194, Sept. 1974

10. G. B. Zimmerman, "Numerical Simulation of the High Density Approach to Laser-Fusion", UCRL-74811, October 17, 1973. Laser Program Annual Report for the Period of July - December, 1973, p. 69.

11. R. A. Haas, H. Shay, et. al. UCRL in preparation.

12. J. M. Kindel, K. Lee, and E. L. Lindman, "Surface-Wave Absorption" Phys. Rev. Lett. 34, 134 (1975).

13. K. G. Estabrook, UCRL in preparation.

"Reference to a company or product name does not imply approval or recommendation of the product by the University of California or the U.S. Energy Research & Development Administration to the exclusion of others that may be suitable."

NOTICE

"This report was prepared as an account of work sponsored by the United States Government. Neither the United States nor the United States Energy Research & Development Administration, nor any of their employees, nor any of their contractors, subcontractors, or their employees, makes any warranty, express or implied, or assumes any legal liability or responsibility for the accuracy, completeness or usefulness of any information, apparatus, product or process disclosed, or represents that its use would not infringe privately-owned rights."

TABLE I CAPTION

Polarimetry data on DT-filled glass microballoons. The degrees of linear polarization p_n/p_s are those measured by the polarimeters looking at light backscattered at an angle of 45° to the North and South beams, repectively. The beam axis and polarimeters were in a plane at a 45° angle to the laser electric field. The polarimeters were rotated about their line-of-sight direction so that if the light were reflected in the geometric optics limit, a degree of linear polarization equal to -1 would be measured. The fraction absorbed is determined either from an array of calorimeters measuring the particle and x-ray energies or from an array of photodiodes mapping the scattered light distribution within the target chamber. Calorimeters measured both the incident beam energies and the light energies reflected and transmitted through the lenses, so the absorbed optical energy could be calculated.

FIGURE CAPTIONS

1. Polarization state of the reflected light for linearly polarized light incident upon a plane-stratified plasma with its electric field polarization vector $\hat{e}$ at an angle Ψ to the scattering plane. (a) In the geometrical optics limit of a long density scale height, $\hat{e}$ is parallelly displaced along the ray trajectory in a non-Euclidean space whose metric is $d\tau^2 = n^2 (dx^2 + dy^2 + dz^2)$. The ray trajectory is itself a geodesic in this space (Fermat's law). The vector $\hat{e}$ will always remain at a constant angle to the scattering plane. (b) In the limit of a very steep density profile, the electron density is considered to discontinuously jump from vacuum to infinitely high density. Since the tangential electric field at the discontinuity must be zero, $\hat{e}$ will be inverted upon reflection so that it projects below the scattering plane by an angle Ψ.

2. Polarimetry of the light backscattered at an angle of 45° to the incident beam for a one-sided ball-on-stalk shot. An incident light ray whose electric vector projects 45° out of the scattering plane changes its polarization state upon reflection, since the TM wave ($\hat{e}$ in the plane) is attenuated and shifted in phase relative to the TE wave ($\hat{e}$ normal to the plane). The transmission axis of the Brewster window also points out of the plane at an angle of 45° and is oriented so that if the target reflects light as a perfectly conducting sphere, the reflected light will be totally transmitted through the Brewster window. The density contours were generated by a LASNEX run modelling target shot #75062506, where an 87.5 μ diameter ball was illuminated by a 14.9 J, 75 ps FWHM pulse focussed by an f/1.1 lens. These contours, computed at the peak of the laser pulse, show no steepening at critical density since LASNEX ignores light pressure.

3. Determination of the density scale length at critical density by polarimetry. The angles θ are measured from the normal in vacuum and the densities are in units of the critical density n_c. Each point represents the result of numerically integrating the wave equations for both polarization states, assuming a plane wave obliquely incident upon a cold, plane-stratified plasma with a density ramp. The phenomenological electron-ion collision frequency ν, which is proportional to the electron density, was chosen to be 0.001 of the circular optical frequency ω at critical density. (a) The phase shift $\delta = \delta_H - \delta_L$ is plotted against the density scale length $L = |d(n/n_c)/dz|^{-1}$ for several incidence angles and density profiles. The degree of linear polarization $p = -\cos\delta$ is that measured by a polarimeter looking at the light scattered in a plane at 45° to the laser electric field and oriented so that $p = -1$ in the geometrical optics limit. The periods of the oscillations in the curves are consistent with interference between reflections from the turning point at $n = n_c \cos^2\theta$ and from the discontinuity in the slope at $z = 0$. (b) The azimuthal asymmetry is plotted against the scale length assuming $n_L = 0.5\ n_c$ and $n_H = 2.0\ n_c$.

The azimuthal asymmetry equals the square of the absolute value of the ratio of the amplitude reflection coefficient of the TM wave to that of the TE wave.

4. In-and out-of-plane polar distributions of the scattered light and particle blowoff energies for the ARGUS two-beam ball-on-stalk shot #36080507, in which two opposing beams of energies 42.4J and 37.6J were focussed upon an 85μ diameter, 0.74μ wall thickness glass shell filled with 2.69 mg/cm^3 equal-molar DT fill. Pulse duration was roughly 35 psec FWHM, giving an intensity of $0.95 \cdot 10^{16}$ W/cm^2.

5. Evidence for azimuthally asymmetric heating of the shell for ball-on stalk shot #56020501 performed on the CYCLOPS two-beam facility with f/2.5 lenses. An 85μ diameter ball was irradiated by two 16.3J, 46 ps FWHM pulses, yielding $0.7 \cdot 10^6$ neutrons. (a) Greater than two to one asymmetry was observed in the side-scattered light. Theta is the angle between the detector line of sight and the beam axis. If this asymmetry is from resonant absorption, those sectors of the shell where the light impinged as a p-polarized wave should be preferentially heated. (b) Time-integrated photographs from the x-ray microscopes are consistent with asymmetric heating. An equivalent-plane photograph of one of the beams at the target plane (photo A) shows it to be nearly circular. The line-of-sight of one x-ray camera lay in the plane of polarization and was at 45° above the beam axis. The image in the 0.8 keV channel (photo B) showed the in-plane sectors to emit x-rays more intensely. Photo C is the image in the 0.8 keV channel for the x-ray microscope looking at the target out of the plane of polarization and at 90° to the beam axis.

6. Time-integrated scattered light distribution averaged over five JANUS two-beam ball-on-stalk experiments. The intensities have been normalized to the total incident light energy and the brackets indicate the one-sigma scatter of the data. Typically, a ball of diameter 83 ± 2 μ diameter and 0.8 ± 0.2 μ wall thickness was irradiated with 34 ± 4 J in 75 ± 25 psec FWHM. The ion calorimeters at $\theta = 45°$ and $\theta = 120°$ saw all of the energy in x-rays and in the particle blowoff, but only a fraction of the light energy, since most was reflected. The light contribution to each calorimeter signal was subtracted off by knowing the scattered light intensity seen by a nearby photodiode.

7. Time-integrated azumuthal distribution of light backscattered at an angle of 26° to the incident beam for lead-glass targets irradiated by a single beam in a pulse of about 80 ps FWHM on the CYCLOPS facility with f/2.5 optics. The diameter of the illuminated area was about 400 μ for both shots.

8. Time-integrated scattered 1.06 μ light distribution for a 10 μ thick tungsten-glass disk illuminated by a single beam of energy 45.6 J and pulse duration 180 ps FWHM on the CYCLOPS facility (Shot #56031901). The intensity on target was $4.4 \cdot 10^{14}$ W/cm^2. An angle of 180° corresponds to direct backscatter.

TABLE I

SHOT NO.	INCIDENT ENERGIES (Joules) (North/South)	ABSORBED ENERGIES (Joules) (Ions/Light)	PULSEWIDTH (psec)	BALL DIA.	NEUTRON YIELD	DEGREE OF LINEAR POLARIZATION (pn/ps)
# 36072909	47/33	16.8/ -	-	-	$7.0 \cdot 10^7$	0.69/ -
# 36080406	6/41	14.2/ -	-	84	$1.3 \cdot 10^7$	0.87/0.77
# 36080507	42/38	8.9/ -	49^{o}	85	$4.0 \cdot 10^7$	0.78/0.83
# 36080611	35/26	11.7/ -	45^{o}	83	$1.5 \cdot 10^8$	0.86/0.87
# 36091310	30/31.4	<14.5/15.4	-	109	$1.2 \cdot 10^8$	0.77/ -
# 36091408	35/19.5	14.6/12.3	26^{n}	83	$1.3 \cdot 10^8$	0.82/ -
# 36091610	57.3/47.4	20.9/17.9	39^{n}	105	$2.2 \cdot 10^8$	0.80/ -
# 36091706	60.9/47.7	19.9/18.5	57^{o}	106	$1.4 \cdot 10^8$	0.79/ -
# 36100812	58.1/37.8	- /28.5	40^{o}	87	-	0.85/ -
# 36100813	48.0/ 0.0	- /13.5	44^{o}	89	-	0.80/ -

o pulse width measured at the oscillator

n pulse width measured at the output of the North arm

POLARIZATION STATE OF THE REFLECTED LIGHT FOR A LINEARLY POLARIZED WAVE OBLIQUELY INCIDENT UPON A PLASMA SLAB

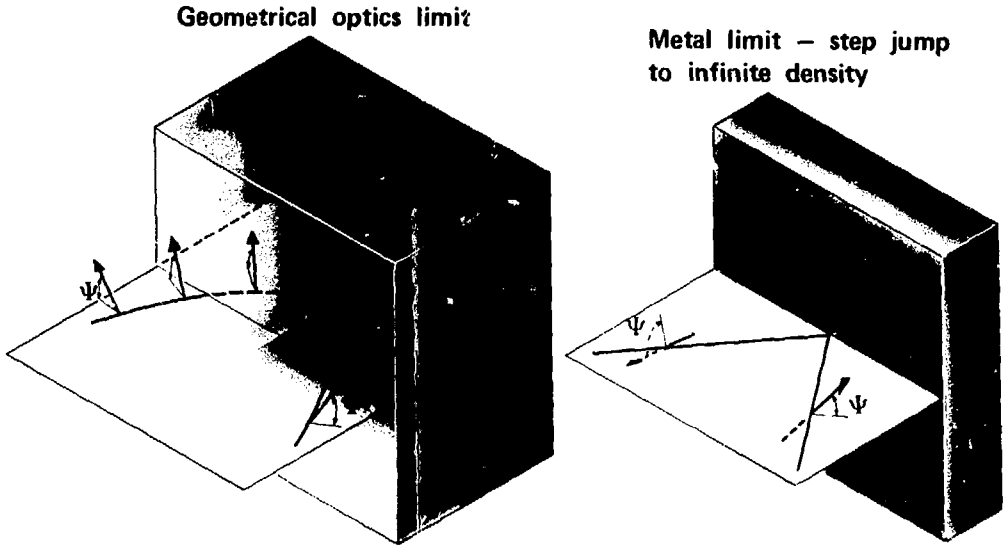

(A)

Electric field polarization vector $\hat{e}$ makes a constant angle with the scattering plane

(B)

Tangential electric field at the discontinuity must be zero

10/76

Figure 1

POLARIZATION MEASUREMENT ON THE SCATTERED LIGHT

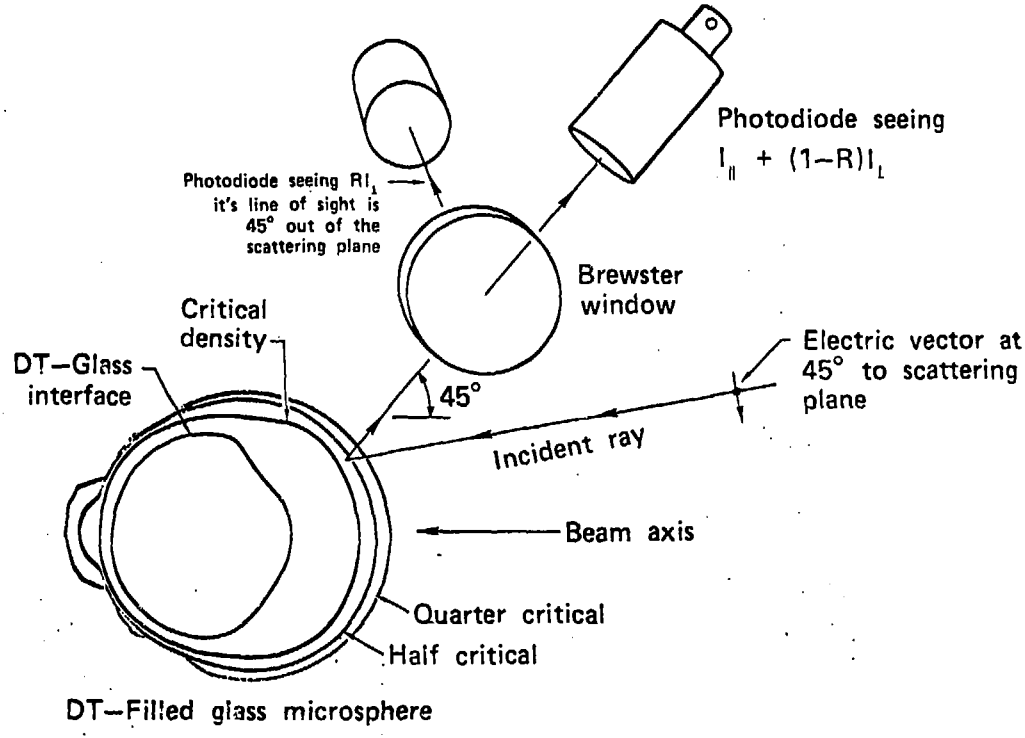

Figure 2

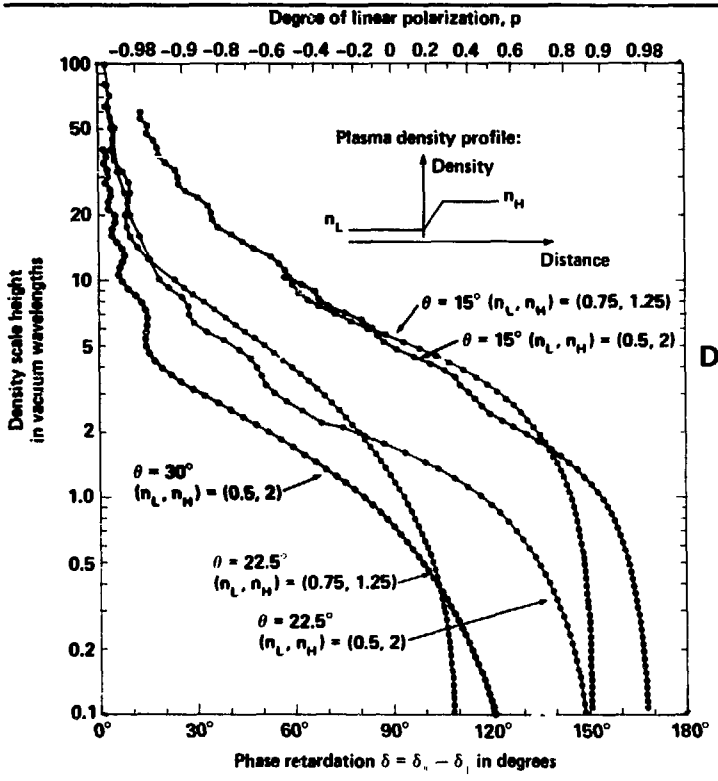

DETERMINATION OF THE SCALE HEIGHT BY POLARIMETRY

Figure 3a

AZIMUTHAL ASYMMETRY OF THE SCATTERED LIGHT DUE TO THE POLARIZATION DEPENDENCE OF RESONANCE ABSORBTION

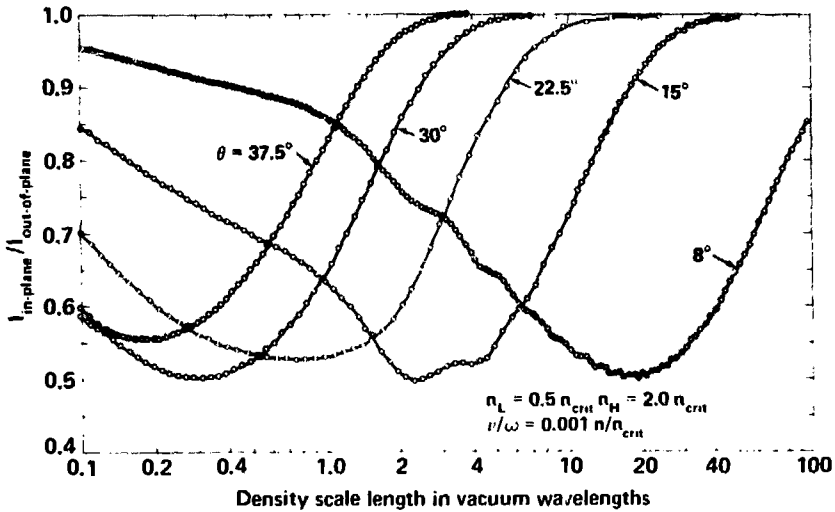

Figure 3b

IRRADIATION OF MICROSHELLS WITH F/1 FOCUSING LENSES SHOW A STRONG POLARIZATION DEPENDENCE OF THE SCATTERED LIGHT AS WELL AS THE PARTICLE AND X-RAY ENERGIES

Shot 36080507: Incident energy 75 J/35ps
Neutron yield 1.5 × 10^8

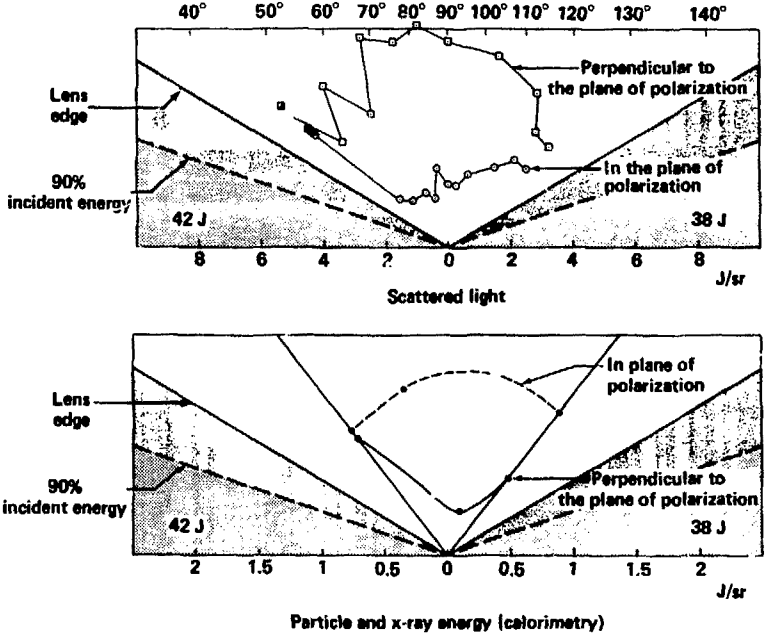

FIGURE 4

SCATTERED 1.06μ LIGHT DISTRIBUTION

Cyclops shot #56020501
85 μ diam. ball, 0.7 million neutrons
16.3 J each beam, 46 psec FWHM

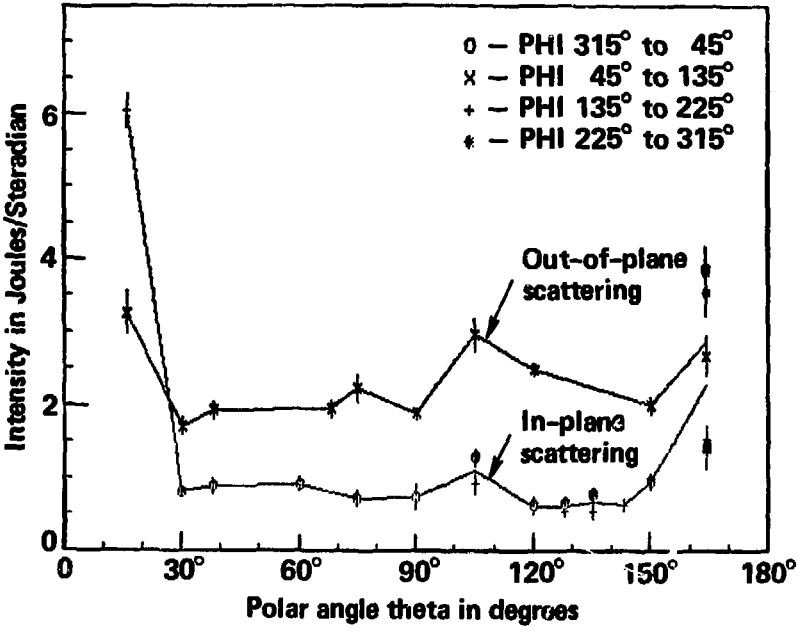

FIGURE 5 (a)

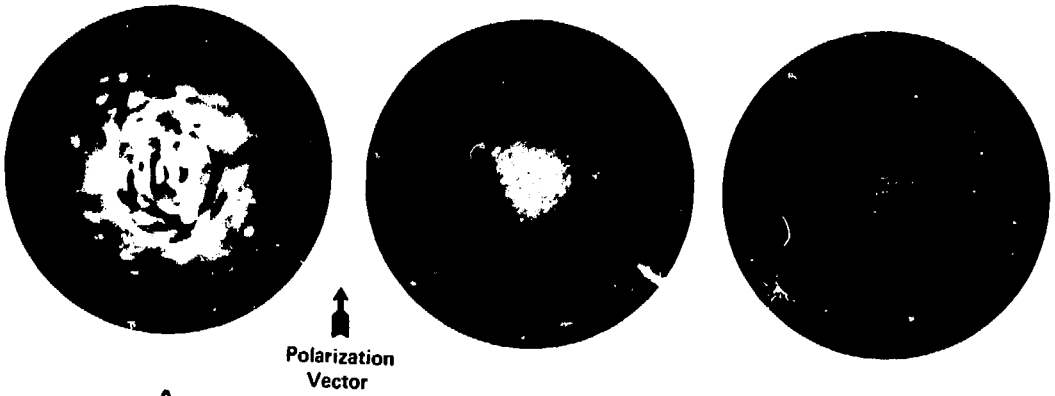

A

Incident beams' intensity distribution

B

.8 keV x-ray emission 45° above beam

C

.8 keV x-ray emission 90° to beam

Figure 5b

AVERAGED SCATTERED 1.06 MICRON LIGHT DISTRIBUTION FOR JANUS EXPERIMENTS ON DT^3He-FILLED GLASS MICROBALLOONS

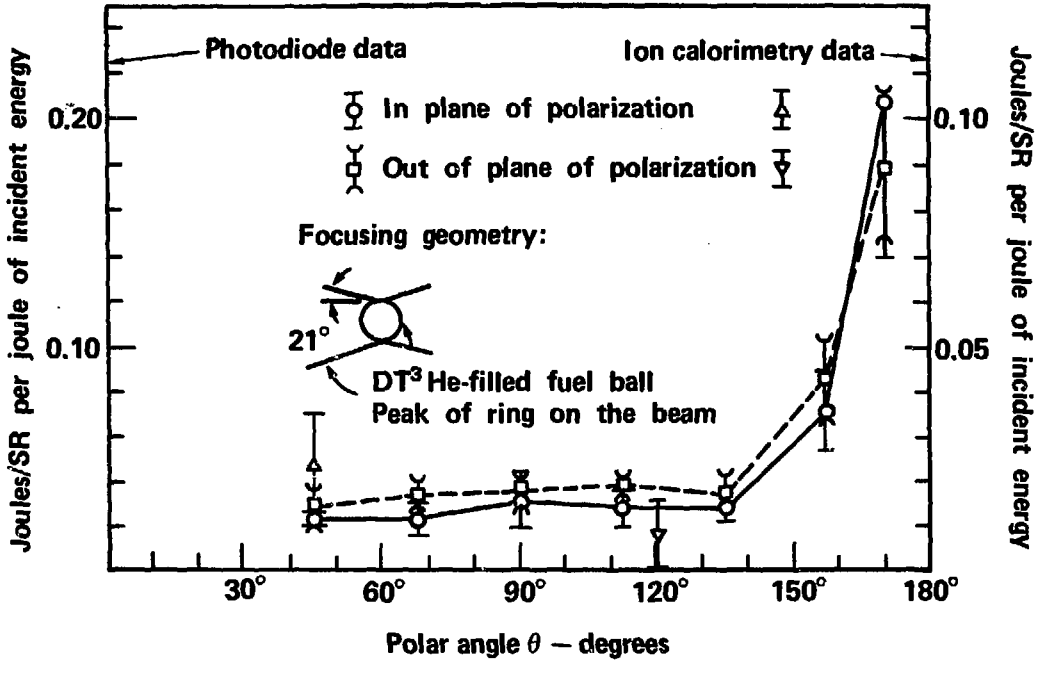

Figure 6

TIME-INTEGRATED AZIMUTHAL DISTRIBUTION OF LIGHT BACK-SCATTERED AT AN ANGLE OF 26° TO THE INCIDENT BEAM FOR LEAD-GLASS TARGETS

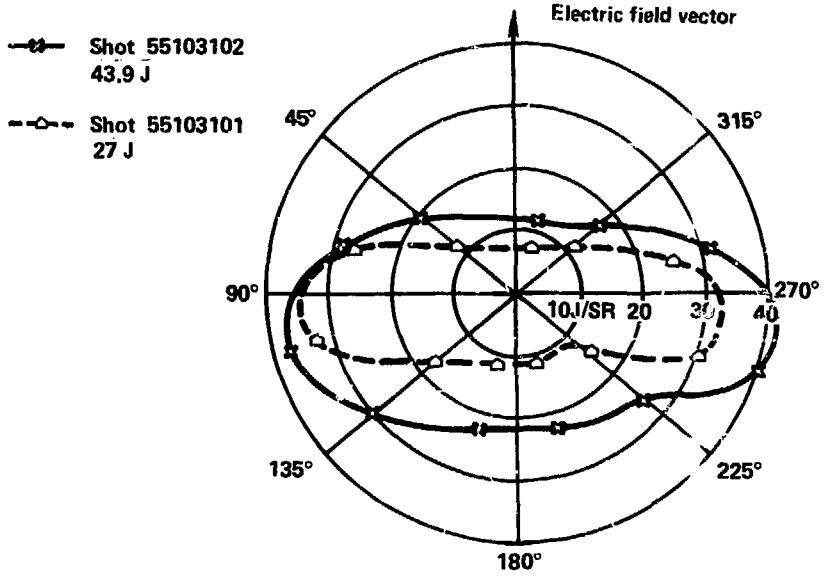

Figure 7

SCATTERED 1.06 μ LIGHT DISTRIBUTION

Cyclops shot #56031901 — 45.6 J, 180 ps FWHM
10 μ thick tungsten-glass disk — $4.4 \cdot 10^{14}$ W/cm^2

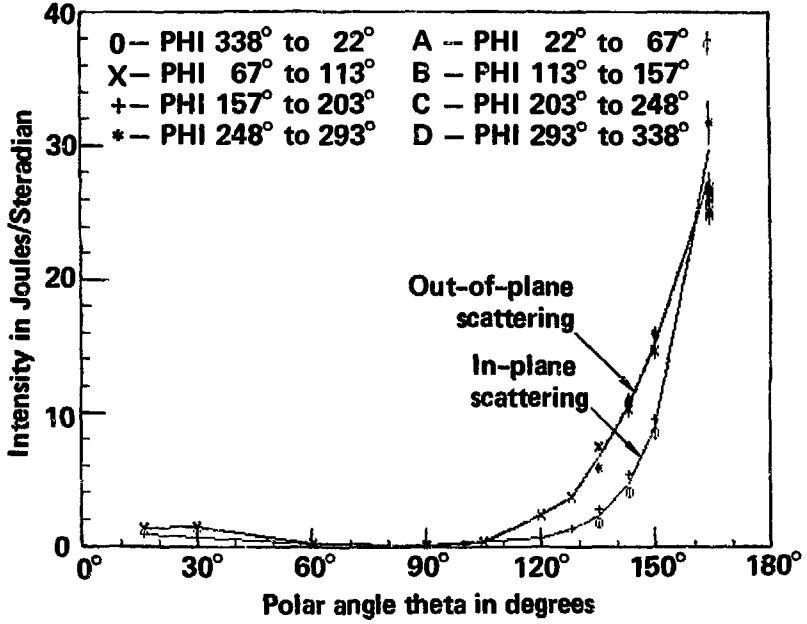

(In-plane points at 60° and 90° are fictitious.)

Figure 8